

**NORTH ATLANTIC TROPICAL CYCLONES:
A KINETIC ENERGY PERSPECTIVE**

A Thesis
Presented to
The Academic Faculty

by

Angela Marcelun Fritz

In Partial Fulfillment
of the Requirements for the Degree
Master of Science in the
School of Earth and Atmospheric Science

Georgia Institute of Technology
August 2009

**NORTH ATLANTIC TROPICAL CYCLONES:
A KINETIC ENERGY PERSPECTIVE**

Approved by:

Dr. Judith A Curry, Advisor
School of Earth and Atmospheric Science
Georgia Institute of Technology

Dr. Robert X. Black
School of Earth and Atmospheric Science
Georgia Institute of Technology

Dr. Yi Deng
School of Earth and Atmospheric Science
Georgia Institute of Technology

Date Approved: July 6, 2009

*To my mom and dad -
thank you for your constant love and support.*

ACKNOWLEDGEMENTS

I wish to thank my group members, James Belanger and Mark Jelinek, not only for help in the completion of this thesis but the support they have given me throughout my graduate career thus far. I would also like to thank my advisor, Dr. Judith Curry, for the encouragement and advice during the entire research process, which not only took a little longer than expected, but also must have changed topic at least three times.

To my friends in EAS who have been with me for three years of science and fun: thank you for keeping it easy and keeping it real. I would also like to extend a special thanks to Arsineh Hecobian for the practical advice she has lent throughout the years, both on the personal and academic level.

TABLE OF CONTENTS

	Page
ACKNOWLEDGEMENTS	iv
LIST OF TABLES	vi
LIST OF FIGURES	vii
NOMENCLATURE	ix
SUMMARY	xi
<u>CHAPTER</u>	
1 INTRODUCTION	1
Integrated Kinetic Energy	2
Traditional Indices Associated With Energy and Potential Destruction	4
2 DATA AND METHODOLOGY	8
Extended Best Track	8
Integrated Kinetic Energy Method	10
Radial Wind Speed Model	11
3 MODEL EVALUATION	18
4 RESULTS AND DISCUSSION	25
Observational, Storm, and Seasonal Scale Results	26
Comparing IKE and PD to Traditional Energy Indices	27
Destructive Potential	30
5 CONCLUSION	41
REFERENCES	43

LIST OF TABLES

	Page
Table 1.1: Saffir Simpson Hurricane Scale. Note: The NHC has removed surge prediction from the operational SSHS beginning with the 2009 North Atlantic Hurricane Season.	7
Table 2.1: Variance explained (R^2) and mean absolute error (MAE) and root mean square error (RMSE) for radii of 34, 50, and 64 knot wins (R34, R50, and R60) in the EBT dataset. Adapted from Demuth et al., 2006.	16
Table 2.2: Storms missing critical wind radii in the EBT database. These storms were not considered in the approach described in this analysis.	16
Table 2.3: Variables necessary for the H2008 radial wind speed model.	17
Table 4.1: Correlation coefficients calculated on the observational scale. All coefficients are significant to 99%.	34
Table 4.2: Correlation coefficients calculated on the seasonal scale. All coefficients were calculated while controlling for duration. Coefficients with ** are significant to 99%, and * are significant to 90%.	34
Table 4.3: Correlation coefficient calculated on the storm scale. All coefficients were calculated while controlling for duration. Coefficients with ** are significant to 99%.	34
Table 4.4: Correlation coefficients between R34 and maximum sustained wind speed, R34 and IKE, and maximum wind speed and IKE for the defined R34 bins. These correlations have been calculated on the observational scale.	34
Table 4.5: Correlation coefficients for IKE, ACE, PD, and PDI on the seasonal and storm scales. Coefficients are calculated while controlling for duration. Coefficients with ** are significant to 99%.	36

LIST OF FIGURES

	Page
Figure 1.1: Example of intensity analysis tools used to create the NHC Best Track for Hurricane Ike (2008). Local date and time are on the x-axis, and intensity (wind speed in knots) is on the y-axis. Here, “Sat” refers to satellite, “AC” refers to aircraft, and “Drop” refers to dropsonde. This figure is adapted from the NHC storm report of Hurricane Ike.	7
Figure 2.1: Illustration of the method to calculate IKE. θ is the azimuth, r is the radius of the storm, and dr is the radius increment over which IKE is calculated.	16
Figure 2.2: NCEP Sea level pressure reanalysis for 1988 to 2008 in hPa.	17
Figure 3.1: USAF Aircraft Reconnaissance “alpha-4 pattern.” The red line signifies the standard flight pattern, and the numbers, 1 through 4, represent the starting, turning, and ending points of the flight.	21
Figure 3.2: Generic vertical wind profile for warm-core lows (thick black line). Wind speed increases on the x-axis, height on the y-axis. AR flights typically cruise at 700 mb or 3000 meters.	21
Figure 3.3: P—W model profiles of radial winds out to R34 (solid) and associated AR profiles (dashed) for Hurricanes (a) Dolly 2008, (b) Dennis 2005, (c) Gustav 2008, and (d) Felix 2007. Wind speeds are given in ms^{-1} and radial distance in km.	22
Figure 3.4: P—W model profiles of radial winds out to R34 (solid) and associated AR profiles (dashed) for Hurricane Dean at category 1, 2, 4, and 5 (a, b, c, d, respectively). Wind speeds are given in ms^{-1} and radial distance in km.	23
Figure 3.5: IKE method used in this study (x-axis) compared against the HRD IKE method for times when it was available in 2008. A log scale is used to increase the magnification of the data at low IKE values. Points labeled “A” and “B” are discussed in the text.	24
Figure 4.1: Time series of maximum wind speeds, IKE, and R34 in Hurricane Ike (2008). Maximum wind speeds (black dashed) are on the left y-axis, and IKE (red) is on the right y-axis in A (top). R34 is in green (B, bottom) in km. Dates is in UTC, with labels at 00 UTC.	32
Figure 4.2: Relationship between (A) R34 and IKE and (B) maximum wind speed and IKE for U.S. landfalling storms from 1988 to 2008. These calculations were done on the observation scale for the time when U.S. landfalling storms were hurricane strength.	33

- Figure 4.3: (A) Time series of ACE (grey) and IKE (red). Y-axes are specific to the variable. (B) Comparison of storm scale ACE and IKE. Values in B have been normalized and controlled for duration. 35
- Figure 4.4: PDF of R34 (A) and RMW (B) in kilometers (bars) compared to theoretical normal distributions (line) with the same mean and standard deviation. Skewness and kurtosis of the data distributions are labeled in the upper right hand corner. 36
- Figure 4.5: (A) Time series of PDI (grey) and PD (blue). Y-axes are specific to the variable. (B) Comparison of storm scale PDI and PD. Values in B have been normalized and controlled for duration. 37
- Figure 4.6: Joint PDF for U.S landfalling storms. Shading represents the number of occurrences, and SSHS categories are labeled and partitioned over the plot in black lines. 38
- Figure 4.7: Comparison of maximum recorded surge heights to IKE (top) and maximum wind speed (bottom) for storms making landfall in the “West Gulf” region (defined in text, illustrated in Figure 4.8). Surge is in feet and maximum winds are in knots. 39
- Figure 4.8: Tracks of storms making landfall in the “West Gulf” region from 1988 to 2008. Only storms which were hurricane status upon landfall and which had recorded surge values were used. Color points represent Best Track times when the cyclone was a tropical depression (TD, green), tropical storm (TS, yellow), hurricane (HR, orange), and major hurricane (MHR, red). The grey lines are the tracks interpolated between the Best Track locations. 40

NOMENCLATURE

ACE	Accumulated Cyclone Energy
AR	Aircraft Reconnaissance
EBT	Extended Best Track
H1980	Holland (1980) Radial Wind Speed Model
H2008	Holland (2008) Radial Wind Speed Model
HRD	Hurricane Research Division
HURDAT	HURricane DATabase
ICKE	Inner Core Kinetic Energy
IKE	Integrated Kinetic Energy
JPDF	Joint Probability Density Function
MAE	Mean Absolute Error
MRV	Modified Rankine Vortex
NCEP	National Centers for Environmental Prediction
NHC	National Hurricane Center
NOAA	National Oceanic and Atmospheric Administration
PD	Power Dissipation
PDF	Probability Density Function
PDI	Power Dissipation Index
P—W	Pressure—Wind Relationship
R^2	Variance Explained
R34	Radius of 34 Knot Winds
R50	Radius of 50 Knot Winds

R64	Radius of 64 Knot Winds
RH	Relative Humidity
RMSE	Root Mean Square Error
RMW	Radius of Maximum Wind Speed
ROCI	Radius of Outer Close Isobar
RV	Rankine Vortex
SFMR	Stepped Frequency Microwave Radiometer
SSHS	Saffir – Simpson Hurricane Scale
SST	Sea Surface Temperature
USAF	United States Air Force

SUMMARY

Towards advancing the indices of hurricane energetics that are associated with potential damage, we develop a new methodology for calculating integrated kinetic energy (IKE) climatology. A simple, observation and dynamical – based radial wind speed model is used with the Extended Best Track dataset to calculate IKE for North Atlantic Hurricanes from 1988 to 2008. The method is evaluated against previous methods of tropical cyclone intensity analysis, and the results are compared to traditional indices in terms of characterizing storm energetics and relating to storm surge. It is shown that the traditional indices are inaccurate measurements of hurricane energetics, and the assumptions that they are based on are not valid. Furthermore, in analyzing storm surge, it is possible that tropical cyclone damage is more strongly correlated with IKE rather than maximum wind speed.

CHAPTER 1

INTRODUCTION

Hurricane Ike of 2008 was a traditional, Cape Verde storm that formed in the eastern North Atlantic. Ike made initial landfall in Cuba as a Category 5 hurricane on the Saffir Simpson Hurricane Scale (SSHS), and final landfall on the Texas coast as a Category 2. The storm reached maximum size two days before final landfall with a gale-force wind radius of 240 nm (444.5 km), and a radius of maximum wind speed of 80 nm (148 km). It intensified a few hours later to 95 knots, and then made landfall on the 13th. Although Hurricane Ike was only a Category 2 when it began to devastate the Galveston coastline, it killed at least 20 people, and is the fourth most destructive hurricane to make landfall in the United States, with damages likely exceeding \$19.3 billion. The challenge is to explain how a Category 2 hurricane can do as much damage as Hurricane Andrew of 1992 or Wilma of 2005, which was the most intense storm of the 2005 hurricane season.

Tropical cyclone intensity is measured utilizing various techniques including satellite-based analysis and aircraft reconnaissance, which utilizes a variety of methods including dropsondes and Stepped Frequency Microwave Radiometer (SFMR) (Figure 1.1). Together, pressure, wind, and sea state information is used in the creation of the “best track” intensity estimate for which the National Oceanic and Atmospheric Administration’s National Hurricane Center (NOAA NHC) is responsible for, and furthermore, is used to categorize storms on the SSHS (Table 1.1). SSHS categories are in turn used as the primary classification technique communicated with the public.

However, as in the case of Hurricane Ike of 2008, there are times when the SSHS and the maximum wind speed estimates do not accurately convey the destructive

FIGURE 1.1: Example of intensity analysis tools used to create the NHC Best Track for Hurricane Ike (2008). Local date and time are on the x-axis, and intensity (wind speed in knots) is on the y-axis. Here, “Sat” refers to satellite, “AC” refers to aircraft, and “Drop” refers to dropsonde. This figure is adapted from the NHC storm report of Hurricane Ike.

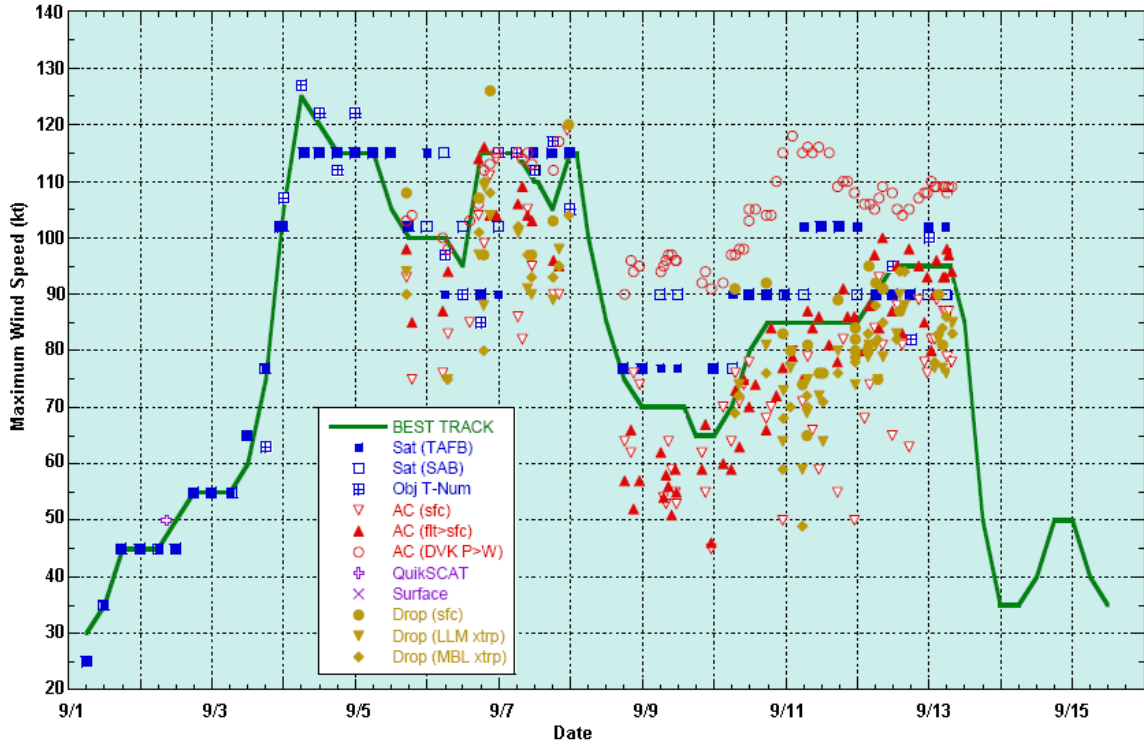


TABLE 1.1: Saffir Simpson Hurricane Scale. Note: The NHC has removed surge prediction from the operational SSHS beginning with the 2009 North Atlantic Hurricane Season.

Type	PC (hPa)	Vm (kt)	Surge (ft)
Tropical Depression	N/A	< 34	N/A
Tropical Storm	< 1000	34 - 63	N/A
Category 1	980 - 1000	64 - 82	4 to 5
Category 2	979 - 965	83 - 95	6 to 8
Category 3	964 - 945	96 - 113	9 to 12
Category 4	944 - 920	114 - 135	13 to 18
Category 5	< 920	> 136	> 19

potential of a tropical cyclone. Although the SSHS warns of potential wind damage, there are other factors that in some storms play a larger role in damage, including storm surge and inland flooding. Kantha (2006) suggests replacing the SSHS with a dynamically-based continuous scale in order to best communicate the potential destruction of a storm. Furthermore, additional intensity indices such as integrated kinetic energy (IKE) have been created (Powell and Rheinhold 2007, Maclay and DeMaria 2008) in response to the need for a better metric to describe a storm's destructive potential. The main difference between IKE and traditional intensity scales is that IKE includes the measure of storm size.

Integrated Kinetic Energy

The Hurricane Research Division (HRD) of the Atlantic Oceanographic and Meteorological Laboratory created an IKE model (Powell and Rheinhold 2007) that uses H*Wind analyses (Powell et al. 1998) in order to integrate kinetic energy over the lifetime of a storm. The calculation is based on wind speeds at 10 meters in the following form:

$$IKE = \int_V \frac{1}{2} \rho U^2 dV \quad (1)$$

where ρ is air density and U is 10 meter wind speed which is integrated over a volume (V) that is defined by the storm's radial extent with a height of 1 meter. The H*Wind analyses used in this calculation have a horizontal and vertical resolution of 6 and 1 kilometers, respectively. H*Wind is available for most tropical cyclones back to 1994 and some prior storms; however, it is primarily dependent on the availability of aircraft

reconnaissance (AR). Furthermore, 2008 is the first season for which the HRD IKE analyses are publicly available.

The benefit of the HRD IKE method is that it relies on a sophisticated wind analysis and therefore provides a high-resolution result, which is particularly desirable when wind radii are not consistent in all four quadrants of the storm. However, it is unable to be extended back in time for climatology studies when storm structure observations from aircraft are unavailable.

Another measure, inner-core kinetic energy (ICKE), has also been suggested (Maclay and DeMaria, 2008), and analysis was performed for the purpose of determining the evolution of kinetic energy throughout the lifecycle of tropical cyclones. ICKE is calculated by integrating the energy for a single air parcel over the volume of the disk (cyclone) and is of the form:

$$\iiint \frac{1}{2} \rho (u^2 + v^2) r dr d\theta dz \quad (2)$$

where u is radial wind, v is tangential wind, ρ is air density, r is radius, θ is azimuth, and z is height. In this study, the radius of maximum wind speed (RMW) is used as the outer radial limit for the model. Maclay and Demaria (2008) suggests a Kinetic Energy Hurricane Scale based on these results; however, the use of the radius of gale – force winds (R34) would be more desirable in an IKE calculation in order to convey a tropical cyclone’s total kinetic energy.

For any form of IKE to be useful in climatology studies, a method is needed that can extend back in time for storms with minimal in situ observations. Here, a method is suggested that utilizes a simple radial wind speed model that can be run using any type of size and intensity measurement, whether aircraft or satellite. For example, given a

consistent measure of storm size from satellite along with historical track data for tropical cyclones, a global climatology of tropical cyclone energy could be created that extends through the satellite era.

Traditional Indices Associated With Energy and Potential Destruction

Traditional methods of tropical cyclone energy assessment include Accumulated Cyclone Energy (ACE; Bell et al. 2000) and the Power Dissipation Index (PDI; Emanuel 2005). These indices have been used not only to evaluate the total tropical cyclone energy of a season, but also to explain the variability of damage in the United States. However, these indices make several assumptions about the nature of storm structure and the variability of storm size on both the storm and seasonal time scales that have not been verified.

ACE is an index that has been used to measure the energy dissipated in a given hurricane season, and is even referred to as a measure of “integrated tropical cyclone energy” (e.g. Maue 2009). ACE is calculated using

$$\int V_{\max}^2 dt \quad (3)$$

where V_{\max} is the maximum 10 meter wind speed of the tropical cyclone, and dt is the time over which it is integrated. This calculation is performed when the cyclone is at least tropical storm strength (maximum sustained winds of 34 knots). ACE originated in the State of the Climate report for 1999 (Bell et al. 2000) as an extension of the Hurricane Destructive Potential index, which is similar to ACE, but integrates the square of the maximum winds for times when a tropical cyclone was hurricane strength.

PDI was suggested (Emanuel 2005) as a way to address the monetary loss in tropical cyclones, as well as to remove the dependence on storm duration in seasonal climatology of tropical cyclone energy. Power dissipation (PD) is defined as

$$PD = 2\pi \int_0^{\tau} \int_0^r C_D \rho |V|^3 r dr dt \quad (4)$$

where C_D is the drag coefficient in the storm, ρ is the air density, V is the wind speed, and r is the radius of the tropical cyclone. In tropical cyclones, V is a function of r . PDI was suggested as an index to represent the power dissipation of the storm:

$$PDI = \int_0^{\tau} V_{\max}^3 dt \quad (5)$$

where V_{\max} is the maximum wind speed of the storm. Emanuel (2005) uses two assumptions to reduce PD to PDI: first, that radial profiles of wind speed in tropical cyclones are geometrically similar, and second, that the size of a tropical cyclone relates little to maximum wind speed. While the second assumption is correct (Merrill 1984), the first assumption has not been sufficiently evaluated.

Towards advancing the indices of hurricane energetics that are associated with potential damage, we develop a new methodology for calculating IKE climatology. This new method requires significantly fewer observations relative to previous methods. It uses the radius of gale-force winds as the outer radius of calculation, which leads to an IKE that is indicative of the total kinetic energy of the storm.

A simple, observation and dynamical –based radial wind speed model is used with the Extended Best Track data set (Demuth et al. 2006) to calculate IKE for North Atlantic Hurricanes from 1988 to 2008. This study evaluates the wind speed model against aircraft reconnaissance wind profiles to justify the approach. The IKE method

presented in this research is then validated against the HRD IKE analyses, and compared to the aforementioned traditional indices of tropical cyclone energy (ACE and PDI). Chapter 2 describes the data used in this study as well as the radial wind speed model and IKE method. Chapter 3 evaluates both the wind speed model and the IKE results against previous methods of tropical cyclone intensity analysis. Chapter 4 illustrates the benefits of IKE relative to traditional indices in terms of characterizing storm energetics and relating to storm surge, and Chapter 5 concludes.

CHAPTER 2

DATA AND METHODOLOGY

The data required for this research include tropical cyclone size and intensity. Information on the size of tropical cyclones is available from satellites, and is virtually nonexistent in official observational records prior to the satellite era. Some information (e.g. radius of outer closed isobar) is available on surface weather maps before 1970, but was only recorded when tropical cyclones were close to landfall. The HURricane DATabase (HURDAT) was created by HRD. HURDAT is the official tracking dataset for the North Atlantic, and contains 6-hourly tropical cyclone location coordinates and maximum 1-minute sustained wind speeds at 10 meters (Neumann et al. 1999). However, size is not included in HURDAT for tropical cyclones before the late 1980s. The Tropical Cyclone Extended Best Track (EBT) dataset (Demuth et al. 2006) was created to supplement the standard HURDAT files with information on storm structure. It extends back to 1988 in the North Atlantic and is used in this study as the source for tropical cyclone intensity and size.

Extended Best Track

A reliable method of determining tropical cyclone intensity and surface wind structure is needed when aircraft reconnaissance (AR) is not used (Demuth et al. 2004). Cases for which a tropical cyclone is not a landfall threat or is outside the Atlantic basin (the East Pacific being the exception) do not receive AR (Weatherford and Gray 1988). In these cases, a subjective approach is used to estimate intensity (Dvorak 1975). While the technique is suitable for purposes of emergency management and preparation, the subjective nature makes studying the climatology of storm size and intensity difficult.

The EBT dataset was compiled as a solution to this problem. It utilizes Advanced Microwave Sounding Unit data, which has been qualified as reliable (e.g. Kidder 1979; Bankert and Tag 2002). EBT is comprised of all the fields that are included in the HURDAT dataset, as well as critical radii of 34, 50, and 60 knot wind (R34, R50, and R64, respectively) in all four quadrants, radius of maximum wind (RMW), eye diameter, radius of outer closed isobar (ROCI), and pressure of outer closed isobar. A modified Rankine vortex approach (Depperman 1947) was used in combination with a vector proportional to storm motion to determine the asymmetric wind structure, which led to the critical radii in the four quadrants.

Cases from the 1999 through 2004 Atlantic hurricane seasons in which there is AR data were used to create and validate EBT. 80 per cent of the cases were used in compiling the best-subsets linear regression models, and 20 per cent were used in validation. Predictors that minimized model error were used in the final EBT model. Model statistics, including variance explained (R^2), mean absolute error (MAE), and root mean square error (RMSE), are listed in Table 2.1. A more complete description of the creation of the EBT dataset can be found in Demuth et al. (2006).

TABLE 2.1: Variance explained (R^2), mean absolute error (MAE) and root mean square error (RMSE) for critical radii in the EBT dataset. Adapted from Demuth et al. (2006).

	R34	R50	R64
R^2	78.4	78.2	86.4
MAE	16.9	13.3	6.8
RMSE	21.4	17.3	8.9

EBT is publicly available from NOAA's Cooperative Institute for Research in the Atmosphere. The dataset is comprised of observational and modeled data for each 6-hour observation at 00, 06, 12, and 18 Coordinated Universal Time (UTC) for every tropical

system from 1988 to 2008, including tropical depressions, tropical storms, hurricanes, tropical waves, tropical disturbances, extra-tropical storms, and remnant lows.

The IKE calculations presented in this study use the EBT maximum wind speed, minimum central pressure, critical wind radii (specifically R34), and translational velocity (determined from latitude and longitude fixes) for times when storms were at least hurricane strength and over open water. This limit was chosen based on the inability of the radial wind speed model to resolve very weak storms, storms over land, and storms that are not tropical in nature (more details regarding the radial wind speed model are discussed later in this chapter). Also, choosing only hurricane-strength cyclones ensured that a majority of the observations times would include critical radii.

Integrated Kinetic Energy Method

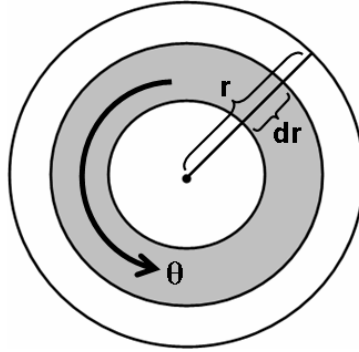
A modified version of the radial wind speed model from Holland (2008) (hereafter H2008) is applied to hurricane-strength storms in the EBT dataset, from which kinetic energy can be calculated. The remainder of this chapter describes in detail the kinetic energy calculation and the radial wind speed model.

The IKE method presented here depends on horizontal distribution of surface wind speed, specifically the radial distribution of the tangential wind. The total IKE calculation is represented in Figure 2.1 using:

$$IKE = \iiint \frac{1}{2} \rho v^2 r dr d\theta dt \quad (6)$$

where ρ is air density, v is the surface wind speed at the specified radius and time step, r is the radius, θ is the azimuth, and t is time.

FIGURE 2.1: Illustration of the method to calculate IKE. θ is the azimuth, r is the radius of the storm, and dr is the radius increment over which IKE is calculated.



For each time step in EBT that a storm is at least hurricane strength, a radial wind speed profile is calculated using the radial wind speed model H2008, from which IKE is calculated via equation (6) with a 1 kilometer resolution along the radius of the storm out to the radius of tropical storm strength winds (R34). IKE can then be integrated over the storm life cycle and furthermore, for all of the storms in a particular season. IKE was calculated for 260 hurricane-strength tropical cyclones in the EBT dataset from 1988 to 2008. Only 7 hurricanes, which lacked critical wind radii, were eliminated from consideration (Table 2.2). With the exception of Helene 1988, these storms were short-lived and inconsequential to this study.

TABLE 2.2: Storms missing critical wind radii in the EBT database. These storms were not considered in the approach described in this analysis.

Season	Name	Max SSHS	Missing Variable
1988	Debby	Cat 1	RMW
1988	Florence	Cat 1	RMW
1988	Helene	Cat 4	RMW
1989	Chantal	Cat 2	RMW
1989	Felix	Cat 1	RMW
1989	Jerry	Cat 2	RMW
1991	Not Named	Cat 3	RMW, Pressure

Radial Wind Speed Model

There are many empirical pressure—wind (P—W) relationships that have been suggested to relate surface winds to the minimum central pressure of a tropical cyclone, of which most are in the cyclostrophic form:

$$v_m = a\Delta p^x \quad (7)$$

where v_m is the maximum wind, Δp is the difference between the environmental pressure and the minimum pressure of the cyclone, and a and x are empirical constants that can be altered to best describe the relationship in certain regions (e.g. Fujita 1971; Atkinson and Holiday 1977). While these P—W models are relatively simple, they capture the cyclone wind field remarkably well (Holland 1980, Harper 2002). A brief description of commonly used radial wind speed models is given here, which include the Rankine Vortex Model, the modified Rankine Vortex Model, Holland (1980), and H2008.

The most commonly used P—W model for tropical cyclones has been the Rankine Vortex model (RV). The RV model is a simple fluid flow model which assumes the inner core velocity is in solid rotation, and the outer velocity is inversely proportional to the radial distance thus conserving angular momentum. Mathematically, the RV is defined as

$$V_\theta = \begin{cases} \frac{V_o r}{R}, & (0 \leq r < R) \\ \frac{V_o R}{r}, & (R \leq r) \end{cases} \quad (8)$$

where V_θ is the velocity in the direction of θ , V_o is the maximum velocity in the vortex, r is the radius at which the velocity is being calculated, and R is the radius of the maximum velocity. This model has been useful in describing the flow of some

atmospheric phenomena (e.g. mesocyclones, tornadoes, tropical cyclones), but is too simple to resolve the highly variable structure of a tropical cyclone.

A modified Rankine Vortex (MRV) was suggested by Depperman (1947) where

$$Vr^{-1} = \text{constant} \quad (9)$$

inside the RMW and

$$Vr^X = D \quad (10)$$

where $X < 1$, and generally lies between 0.4 and 0.6. The MRV approach requires a very close approximation of the RMW. Without such measurements, the MRV could substantially underestimate the maximum winds in a tropical cyclone because the general profile of the radial winds is calculated incorrectly (Holland 1980).

Holland 1980 (hereafter H1980) describes a model that is based on an extension to the approach of Schloemer (1954). The model follows basic gradient wind speed approximation with a β -parameter, which enables variation in the intensity of pressure gradient near the RMW, and is defined as:

$$V_g(r) = -\frac{rf}{2} + \left[\frac{r^2 f^2}{4} + A\beta(p_n - p_c) \frac{\exp(A/r^\beta)}{\rho r^\beta} \right]^{1/2} \quad (11)$$

where V_g is the wind speed at some radius r , f is the Coriolis parameter, β is the parameter which is used to determine the shape of the profile, p_n is the environmental pressure outside the tropical cyclone, p_c is the central pressure of the tropical cyclone, and ρ is air density. A is another scaling parameter and is defined as

$$A = RMW^\beta. \quad (12)$$

The H1980 model was found to be in close agreement with AR profiles of Cyclones Tracy (1974) and Kerry (1979). The H1980 model is not able to resolve

supergradient winds at the RMW, and it is suggested that direct observation of maximum winds be used whenever possible.

Holland (2008) developed a parametric equation for the β -parameter that can be applied to the H1980 model. This parameter was derived first empirically and then corrected for latitude, storm development, and translational speed. The β definition is

$$\beta = -4.4 \times 10^{-5} \Delta p^2 + 0.01 \Delta p + 0.03 \frac{\partial p_c}{\partial t} - 0.014 \phi + 0.15 V_t^x + 1.0, \quad (13)$$

$$x = 0.6 \left(1 - \frac{\Delta p}{2154} \right), \quad (14)$$

$$v_m = \left(\frac{\beta}{\rho e} \Delta p \right)^{1/2} \quad (15)$$

where ρ is air density, derived from the equation of state, e is the base of natural

logarithms, Δp is the pressure drop to the cyclone center in hPa, $\frac{\partial p_c}{\partial t}$ is the intensity

change in hPa h⁻¹, ϕ is the absolute value of latitude in degrees, and V_t is the translational velocity of the tropical cyclone. This relationship shows that for a given central pressure, the maximum wind speed can vary depending on prior intensity changes, latitude, translational velocity, and air density.

The method used in this paper is based on H1980 and H2008 with some modifications (Personal correspondence: Greg Holland, 2008). In the modified version used here, given a RMW and an outer wind observation, the profile can be constrained by observations by allowing the exponent (x) to vary. For example, the standard exponent based on the application of the cyclostrophic wind relationship is $x = 0.5$. By allowing the exponent to vary based on observations, the profile will fit the peak of the maximum

wind, but will not be in balance with the pressure gradient. This is an advantage over the RV and MRV models that could not resolve strong wind speed gradients at the RMW.

The variables necessary for H2008 are listed in Table 2.3. Translational velocity, V_t , was determined from the EBT latitude and longitude by using a great-circle distance relationship and dividing by the time-step (6-hours):

$$V_t = \frac{R \cdot \arccos(\sin \varphi_i \sin \varphi_f + \cos \varphi_i \cos \varphi_f \cos \Delta\lambda)}{\Delta t} \quad (16)$$

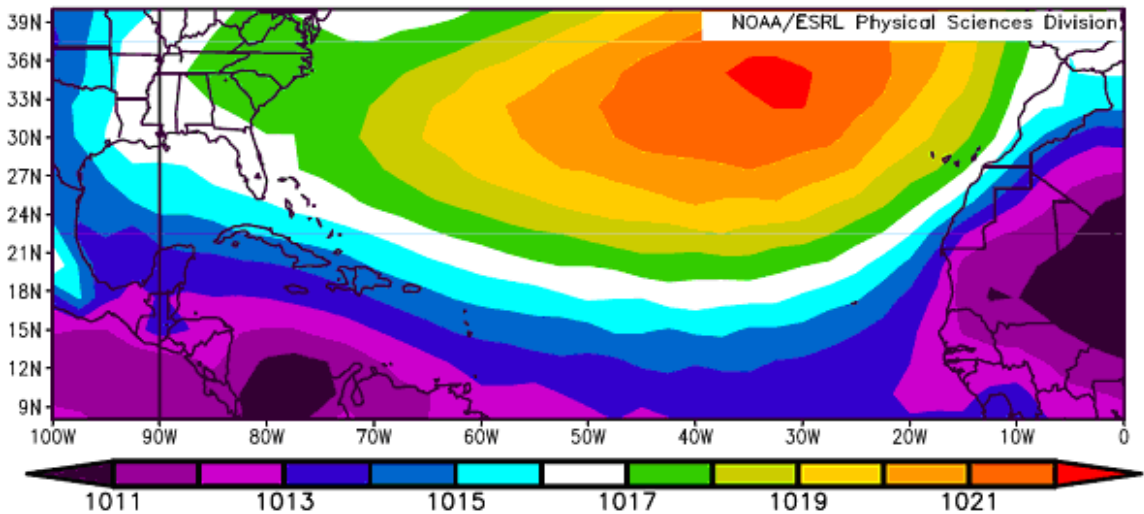
where d is the arc length, R is the radius of the earth (6378 km is used in all cases), φ_i and φ_f are the initial and final geographical latitudes, respectively, and $\Delta\lambda$ is the difference between the initial and final longitudes. Radial wind speed profiles are not calculated for the first observation of each hurricane-strength storm in the EBT dataset.

TABLE 2.3: Variables necessary for the H2008 radial wind speed model.

Variable	Description	Source or assumption
V_m	Maximum winds	EBT
R34	Radius of 34-knot winds	EBT
RMW	Radius of maximum wind	EBT
LAT	Latitude	EBT
LON	Longitude	EBT
P_c	Central pressure	EBT
RH	Relative humidity at RMW	0.9, assumed
SST	Sea surface temperature	27.5°C, assumed
VCG	Velocity of outer V_m observation	34 knots
P_n	Environmental pressure	Climatology (Figure 2.2)
T	Temperature	SST - 1
P_{cm}	Surface pressure at RMW	$P_n - (P_n - P_c)e^{-1}$
q_m	Vapor pressure at RMW	Moist ideal gas law
T_v	Virtual temperature at RMW	Moist ideal gas law
ρ_m	Density of air at RMW	Moist ideal gas law

Environmental pressure is assigned based on climatology from the National Centers for Environmental Prediction (NCEP) Reanalysis Data Set (Kalnay et al. 1996) which is publicly available. Climatology was taken for years 1988 to 2008 (Figure 2.2), and averaged in 5 degree latitudinal bands which was then supplied to the model based on storm location. SST was estimated to be 27.5° C in all cases. No attempt is made to account for storm life cycle variations or seasonal variations in SST. Assuming SST varies ± 2 degrees, this assumption has a negligible impact on wind speed profiles (not shown). Lastly, relative humidity (RH) at the RMW was held constant at 90% for all cases. While RH does vary across the main development region as well as within a tropical cyclone, variations (especially in the eye wall) will tend to be small and have negligible impact on wind speed profiles.

FIGURE 2.2: NCEP sea level pressure reanalysis for 1988 to 2008 in hPa.



For each 6-hour storm observation, a radial wind speed profile is calculated to fit the recorded maximum wind speed, RMW, and R34. The radial wind speed profile and the subsequent kinetic energy are integrated from the storm center out to R34. This radius was chosen over other tropical storm size conventions (e.g. ROCI, the radius

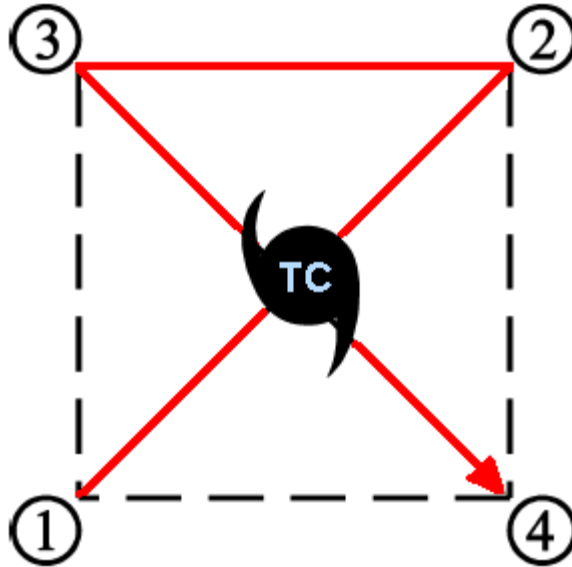
where relative vorticity goes to zero, or RMW) for several reasons. First, R34 estimates are readily available in the EBT dataset for North Atlantic tropical cyclones back to 1988. Furthermore, R34 can be considered the boundary between the vortex and its environment, i.e. the boundary between environmental wind speeds and tropical storm strength wind speeds.

CHAPTER 3

MODEL EVALUATION

AR and the HRD IKE analyses are used to evaluate the wind speed model and IKE method presented in this research. Holland (2008) validates a version of the radial wind speed model against the Dvorak technique (Dvorak 1974) as well as other wind P—W relationships. In this study we evaluate the shape of the profile against in situ AR flight-level measurements. The United States Air Force (USAF) is charged with obtaining wind observations for tropical cyclones in the North Atlantic and the East Pacific for NHC. Using a WC-130J aircraft, their mission is to obtain “center fixes” and maximum wind speeds in the storm. They fly an “alpha – 4” pattern (Figure 3.1) that

FIGURE 3.1: USAF AR “alpha – 4” pattern. The red line signifies the standard flight pattern, and the numbers, 1 through 4, represent the starting, turning, and ending points of the flight.

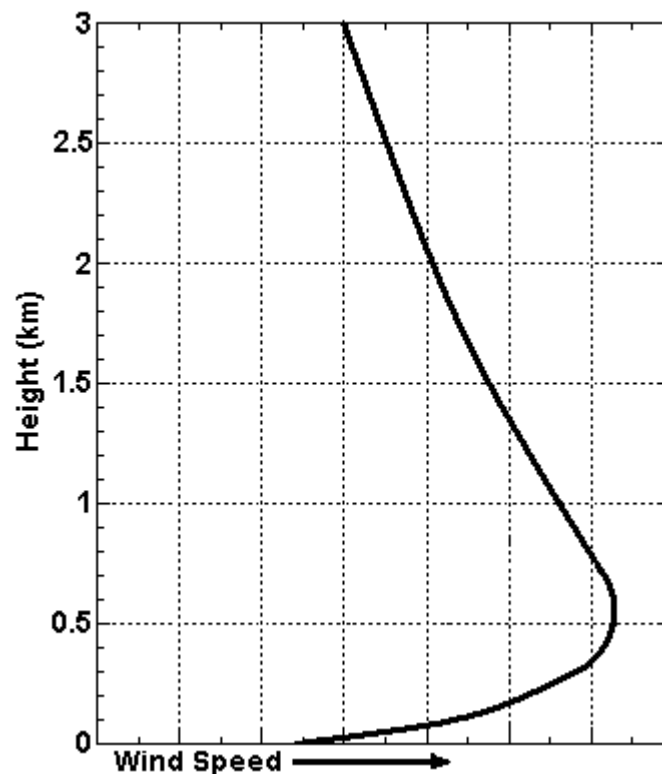


allows them to pass through the center of the storm at least twice per mission. It is rare that a USAF AR flight will fly with a leg distance of more than 105nm (approximately 195 km), and for this reason, evaluation of a wind speed model that extends to the R34 is

difficult (U.S. D.O.C., 2008). These flights typically fly at an altitude of 700 hPa, and all AR profiles used here were obtained at this level.

The relationship between flight-level winds and 10 meter winds is not intuitive. The vertical profile of the radial winds shows an increase up to the level of maximum wind speed (typically 850 hPa) and then decreases above that. This phenomenon is due to a weakening of the radial pressure gradient, indicative of a warm core system (Powell and Black, 1990). Therefore, wind speeds at the AR flight level are comparable to 10 meter winds (Figure 3.2), and in some cases could even be weaker.

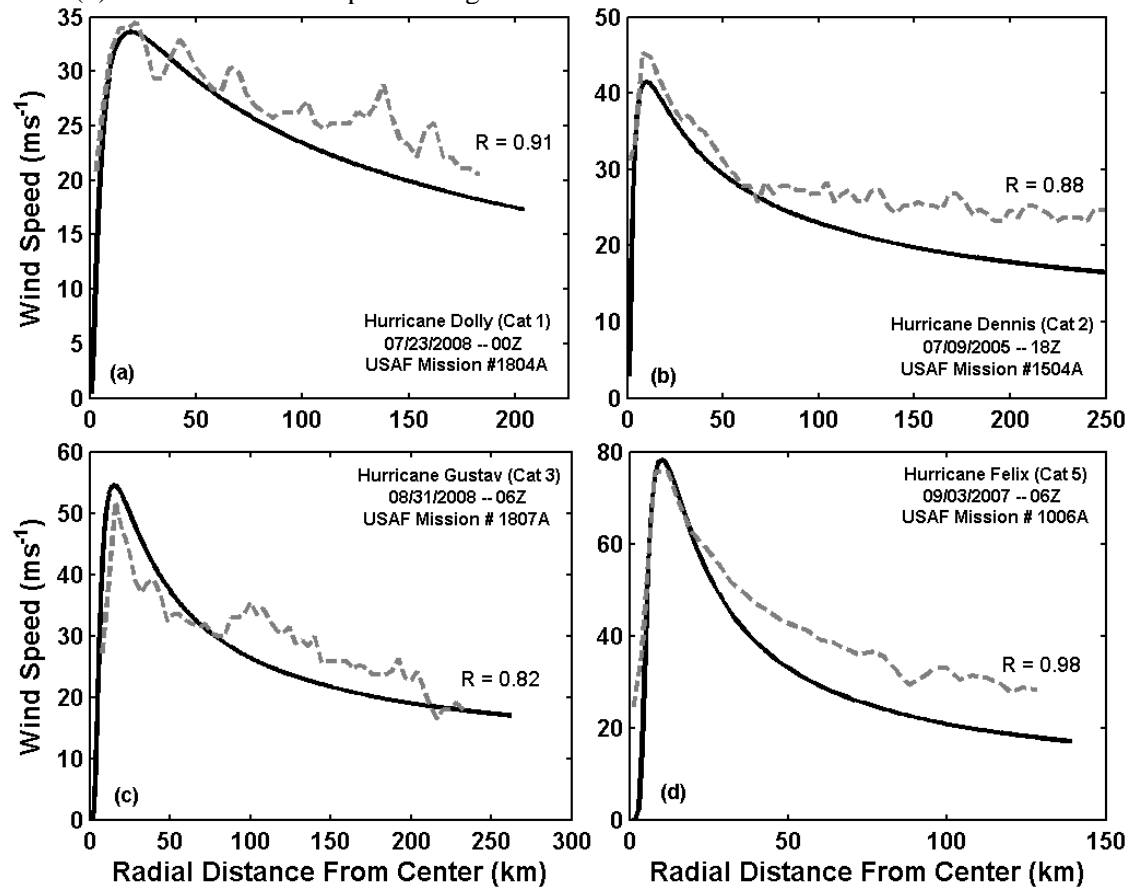
FIGURE 3.2: Generic vertical wind profile for warm-core lows (thick black line). Wind speed increases on the x-axis, height on the y-axis. AR flights typically cruise at 700 mb or 3000 meters.



Four tropical cyclones were chosen to illustrate the model's performance at various intensities (Figure 3.3), and four instances of Hurricane Dean (Figure 3.4) were

chosen to illustrate the model's performance for one storm at different intensities. Dean is an interesting case because of the high number of AR missions sent into the storm and also the time spent at each of the SSHS categories, which enable the radial wind profiles to be calculated accurately.

FIGURE 3.3: P—W model profiles of radial winds out to R34 (solid) and associated AR profiles (dashed) for Hurricanes (a) Dolly 2008, (b) Dennis 2005, (c) Gustav 2008, and (d) Felix 2007. Wind speeds are given in ms^{-1} and radial distance in km.

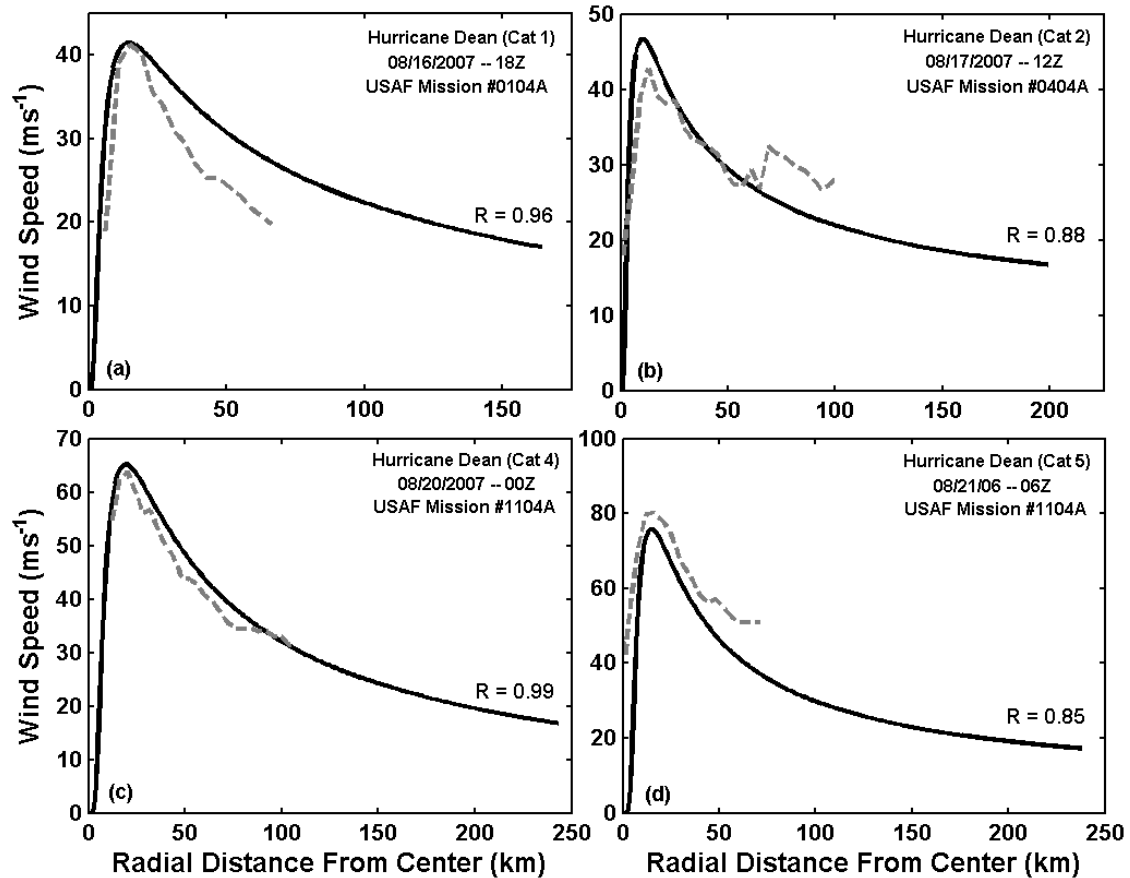


The correlation coefficient was calculated between the model and AR profiles for radius up to 100 km, if available. Of the cases shown, the average coefficient is 0.91. All cases are significant to a p-value of 0.01.

Figure 3.3 illustrates the inability to validate the model past a radius of approximately 75 km. It is especially apparent in the cases of Hurricane Dennis (Figure 3.3b) and Hurricane Gustav (Figure 3.3c) that at this radius, the aircraft began to turn for

the next leg of the mission, at which point the AR profile plateaus. This feature was present in all of the cases that were examined, including those not shown. Verification profiles for Hurricane Dean (Figure 3.4) were not plotted further than the radius where it began to plateau.

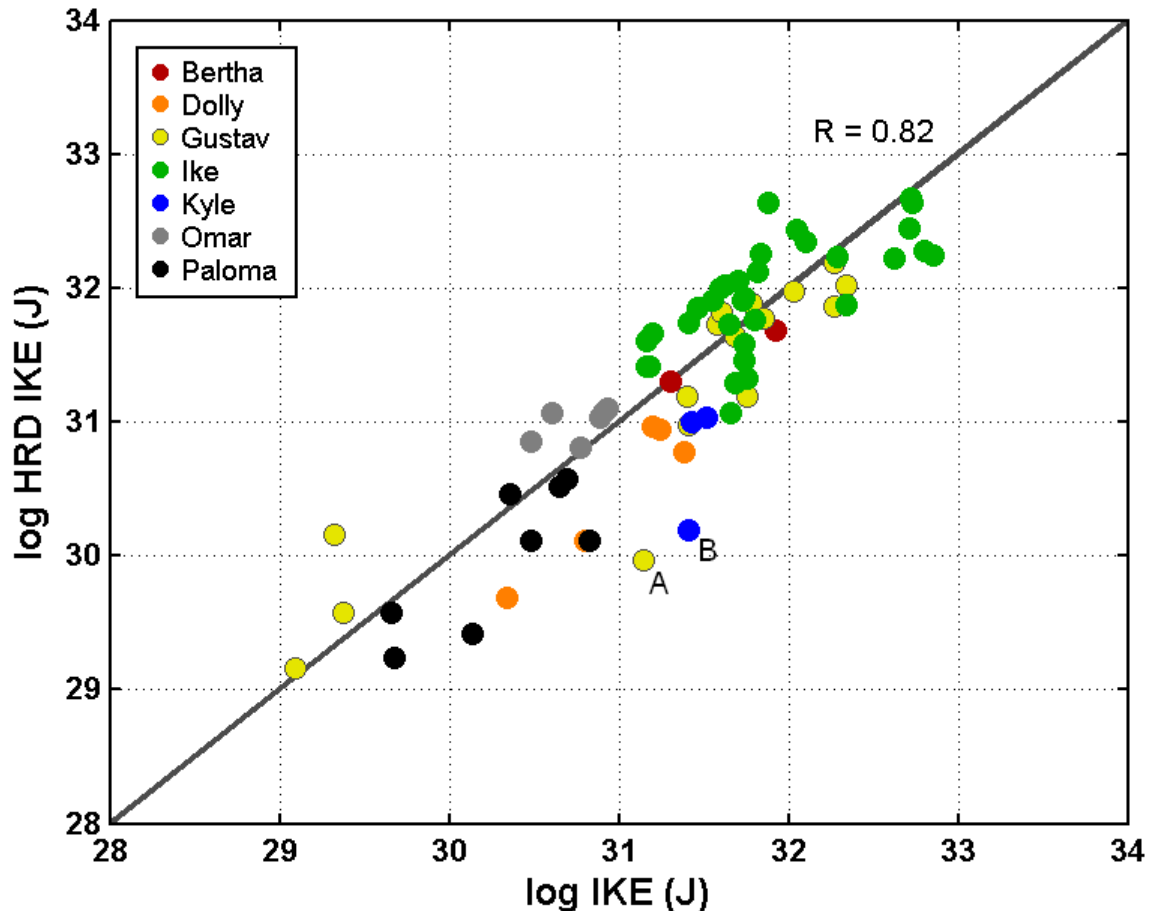
FIGURE 3.4: P—W model profiles of radial winds out to R34 (solid) and associated AR profiles (dashed) for Hurricane Dean at category 1, 2, 4, and 5 (a, b, c, d, respectively). Wind speeds are given in ms^{-1} and radial distance in km.



To assess the performance of the IKE method developed here, the HRD analyses of IKE were compared for all cases from 2008 in which the HRD IKE analysis is available (Figure 3.5). These included Hurricanes Bertha, Dolly, Gustav, Ike, Kyle, Omar, and Paloma. The variance of HRD IKE explained by this study's IKE method is 67%, which is significant to a P-value of 0.01.

Two examples of outliers in this relationship are associated with Hurricanes Gustav and Kyle (labeled “A” and “B”). The Gustav case occurred on August 29th and 18Z around the time the storm is passing over the island of Puerto Rico. The P—W model used in this study does not perform well over land. While these instances are rare in the results, there are some times, especially in the Caribbean, that storms are interacting with land and the model will not perform well. The second example, Kyle, is on September 28th at 00Z, when Kyle was at 35.3° N and slightly extra-tropical. This suggests that the P—W relationship does not match with how HRD analyzed the wind field.

FIGURE 3.5: IKE method used in this study (x-axis) compared against the HRD IKE method (y-axis) for hurricanes in 2008. A log scale is used to increase the magnification of the data at low IKE values. Points labeled “A” and “B” are discussed in the text.



Overall, the model performs well compared to AR winds and the HRD IKE analysis method. The inability of AR to capture R34 diminishes the utility of the HRD IKE analysis in evaluating the new IKE calculations. However, Best Track maximum wind speeds are used in the EBT dataset, to which the radial wind speed model is fit. For this reason there is a high level of confidence that the radial wind speed model is accurately determining the shape of the wind profiles. Figure 3.5 illustrates that the new IKE method excels when systems are purely tropical in nature and entirely over water. Drawbacks to the new IKE method are that the radial wind speed model does not excel when the interaction between land masses and tropical cyclones is strong, and when systems are in the transitional period between tropical and extra-tropical. A latitudinal cutoff could be implemented, since the Coriolis force tends to enlarge cyclones beyond “tropical” sizes as they travel northward.

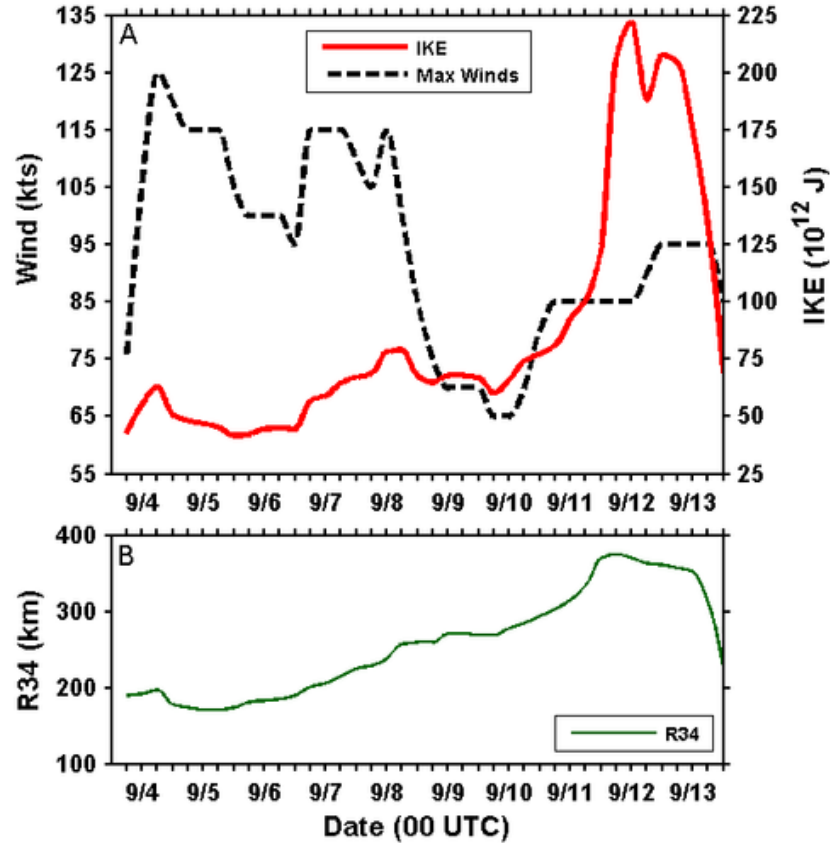
CHAPTER 4

RESULTS AND DISCUSSION

IKE was calculated for all hurricane-strength observations in the EBT dataset from 1988 to 2008, which includes 139 storms. The analysis of the IKE method focuses on the climatology of IKE, the utility of IKE in the analysis of storm energetics, and the utility of IKE in interpreting hurricane destructive potential.

An example of the importance of hurricane size in determining IKE is illustrated using Hurricane Ike of 2008. Hurricane Ike was a large storm upon landfall, with a large IKE value and mean R34 of 375 km. The temporal variability Hurricane Ike's maximum sustained wind speed and IKE are depicted in Figure 4.1. The first 5 days of Hurricane Ike are characterized by very little variability in IKE and strong maximum sustained wind values. While Hurricane Ike was at its maximum intensity, it was also at its lowest IKE. Even though the cyclone was at maximum intensity at this point, it was also in its most compact state. After making landfall on and passing over Cuba (02 UTC on September 8th), Hurricane Ike grew in size and, since wind speeds were still relatively strong, kinetic energy increased. It can be seen that although the maximum wind speed continued to decrease during residence over the Gulf of Mexico, IKE increased to a maximum just prior to landfall at 07 UTC on September 13th. The actual maximum in IKE occurred just before the hurricane begins to interact with land on September 12th, at which point it began to decrease.

FIGURE 4.1: Time series of maximum wind speeds, IKE, and R34 in Hurricane Ike (2008). Maximum wind speeds (black dashed) are on the left y-axis, and IKE (red) is on the right y-axis in A (top). R34 is in green (B, bottom) in km. Dates are in UTC, with labels at 00 UTC.



It is hypothesized that Hurricane Ike became so large because of its track over Cuba, where land interaction acted to both decrease the intensity of the storm, while increasing the aerial size (McWilliams, 1984). This theory is discussed more later in this chapter. It is probable that Ike's size led to the incredible destruction that occurred upon landfall on Galveston Island.

In the discussion that follows, *observational scale* refers to instantaneous measurements (ie. 6-hourly observations). The *storm scale* refers to integration over time when the cyclone was a hurricane. Finally, the *seasonal scale* refers to the integration of hurricane-strength observations over the entire season.

Observational, Storm, and Seasonal Scale Results

Figure 4.2 and Table 4.1 show the relationship between IKE and wind speed and R34 for U.S. landfalling hurricanes. The radius of gale-force winds (R34) explains 67% of the variance in IKE on a seasonal scale after controlling for the affects of duration. This relationship is statistically significant to 99 per cent. Figure 4.2A portrays a quadratic relationship between IKE and R34, which is expected after the integration of

TABLE 4.1: Correlation coefficients between R34 and wind speed and the various energetics indices use in this study. Coefficients are calculated on the observational scale. All coefficients are significant to 99%.

	IKE	ACE	PD	PDI
R34	0.94	0.23	0.82	0.20
V _m	0.29	0.99	0.53	0.98

equation (12). This relationship is heteroskedastic with increasing size. A hypothetical explanation for the heteroskedasticity is that as radius increases, the relationship between wind and IKE becomes stronger, which causes a lesser impact from R34 at larger sizes. However, when the correlation coefficients were calculated after separating the data into increments of size (Table 4.2), it became apparent that the relationship between size and wind speed is variable. Table 4.2 contains the correlation coefficients between wind and R34 after separating the values into radius bins, the coefficients between IKE and R34, as

TABLE 4.2: Correlation coefficients between R34 and maximum sustained wind speed, R34 and IKE, and maximum wind speed and IKE for the defined R34 bins. These correlations have been calculated on the observational scale.

R34 Range	R34, V _m	R34, IKE	V _m , IKE
<150 km	0.24	0.82	0.69
150 - 250 km	0.35	0.83	0.64
250 - 350 km	0.01	0.74	0.44
> 350 km	-0.08	0.48	0.39

well as IKE and maximum wind speed. It can be seen that as cyclone radius increases, the relationship between IKE and both R34 and maximum wind speed decreases.

Furthermore, a conclusion of Merrill (1984) was that there is a weak relationship between size and intensity ($R = 0.34$). However, when doing the same analysis with the EBT dataset form 1988 to 2008, it can be seen that this relationship is not homoskedastic with increasing size.

FIGURE 4.2: Relationship between R34 and IKE (A) and maximum wind speed and IKE (B) for U.S. landfalling storms from 1988 to 2008. These calculations were done on the observation scale for the time when U.S. landfalling storms were hurricane strength.

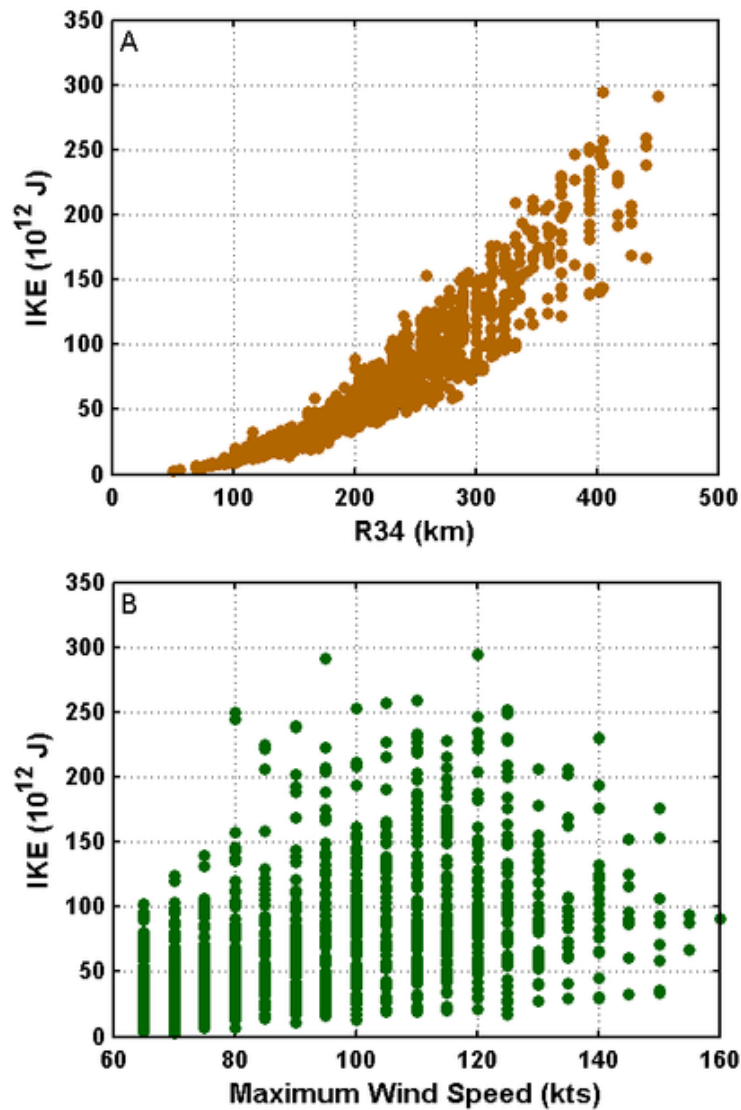


Figure 4.2B illustrates the relationship between IKE and maximum sustained wind speeds on the observational scale for U.S landfalling hurricanes. Immediately one can see that observations with moderately strong wind speeds are exhibiting the highest values of IKE, indicating that cyclone size is playing a larger role than wind speed in IKE. While the correlation between wind speed and IKE is moderate ($R = 0.29$, Table 4.1), the strong relationship between R34 and IKE ($R = 0.94$, Table 4.1) indicates that size is the dominant control on IKE values on the observational scale.

Storm scale correlations (controlling for duration) are listed in Table 4.3. Size again explains the most variance in both IKE and PD on the storm scale. Although

TABLE 4.3: Correlation coefficients calculated on the storm scale. All coefficients were calculated while controlling for duration. Coefficients with ** are significant to 99%.

	IKE	ACE	PD	PDI
Mean R34	0.64**	0.00	0.54**	-0.01
Max R34	0.62**	-0.07	0.48**	-0.07
Mean V_m	0.16	0.78**	0.3	0.76**
Max V_m	0.05	0.57**	0.14	0.57**

significant to 99 per cent, the correlation coefficient between ACE and mean wind speed is only 0.78, and 0.76 for PDI. Furthermore, the correlation between mean wind speed and storm scale IKE is 0.16 (significant to 90 per cent), and while it is still a small value, it shows that wind speed is indeed controlling some of the variability in IKE along with size, whereas duration and wind speed are controlling all of the variability in ACE. Similar results are portrayed in Table 4.4, where seasonal scale correlation coefficients are listed. Both size and wind speed have roles in seasonal IKE, whereas wind speed is the variable responsible for ACE and PDI.

TABLE 4.4: Correlation coefficients calculated on the seasonal scale. All coefficients were calculated while controlling for duration. Coefficients with ** are significant to 99%, and * are significant to 90%.

	IKE	ACE	PD	PDI
Mean R34	0.81**	-0.07	0.74**	-0.10
Max R34	0.44*	0.22	0.36	0.20
Mean V_m	0.18	0.82**	0.12	0.81**
Max V_m	-0.16	0.66**	0.02	0.67**

Comparing IKE and PD to Traditional Energy Indices

Figure 4.3 illustrates the comparison between IKE and ACE on both the seasonal (A) and storm scale (B). Figure 4.3b shows the relationship between IKE and ACE when controlling for storm duration. The data in this figure has been normalized by removing the mean and dividing by the standard deviation. The correlation between these two variables is $R = 0.30$ (Table 4.5). This result is once again a product of IKE being controlled by size. Although duration plays a role in the storm scale comparison between ACE and IKE, the inclusion of size in the energy calculation reduces the variability explained by duration to 70%.

The time series of seasonal IKE and ACE is illustrated in Figure 4.3A as well as Table 4.5. Note that in Figure 4.3A, the y-axes are specific to the variable, and the ACE in these figures are calculated only when storms are hurricane strength in order to be comparable to the IKE calculation. Duration plays a large role in both ACE and IKE on the seasonal scale. The conclusion can be drawn that IKE and ACE are in fact different on seasonal time scales, which is also evident in the correlation coefficient of 0.02 (Table 2.2). It is important to note years where ACE increases and IKE decreases, or *vice versa* (e.g. 1995 to 1996, 2004 to 2005, and 2006 to 2007). This result suggests that for

FIGURE 4.3: (A) Time series of ACE (grey) and IKE (red). Y-axes are specific to the variable. (B) Comparison of storm scale ACE and IKE. Values in B have been normalized and controlled for duration.

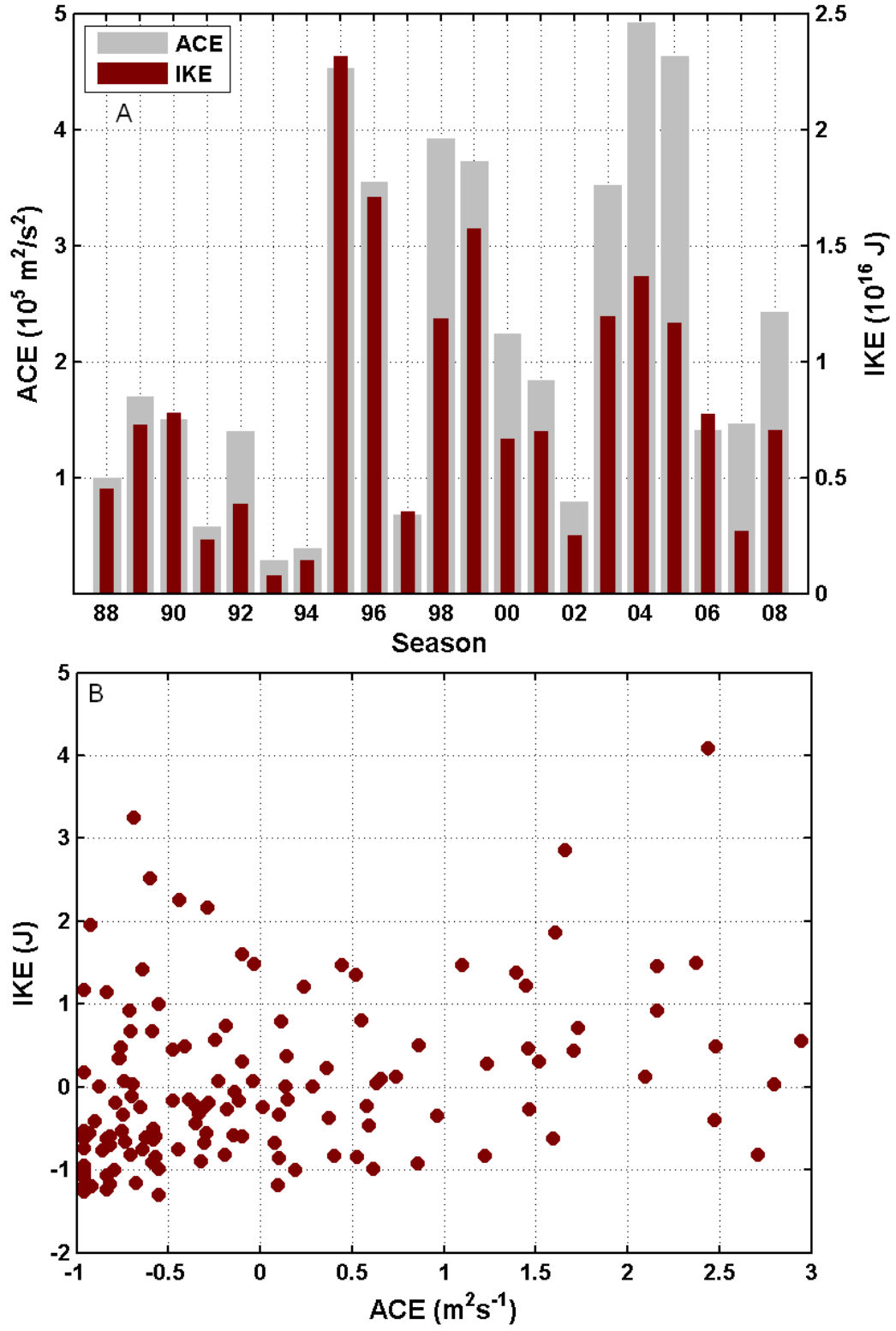
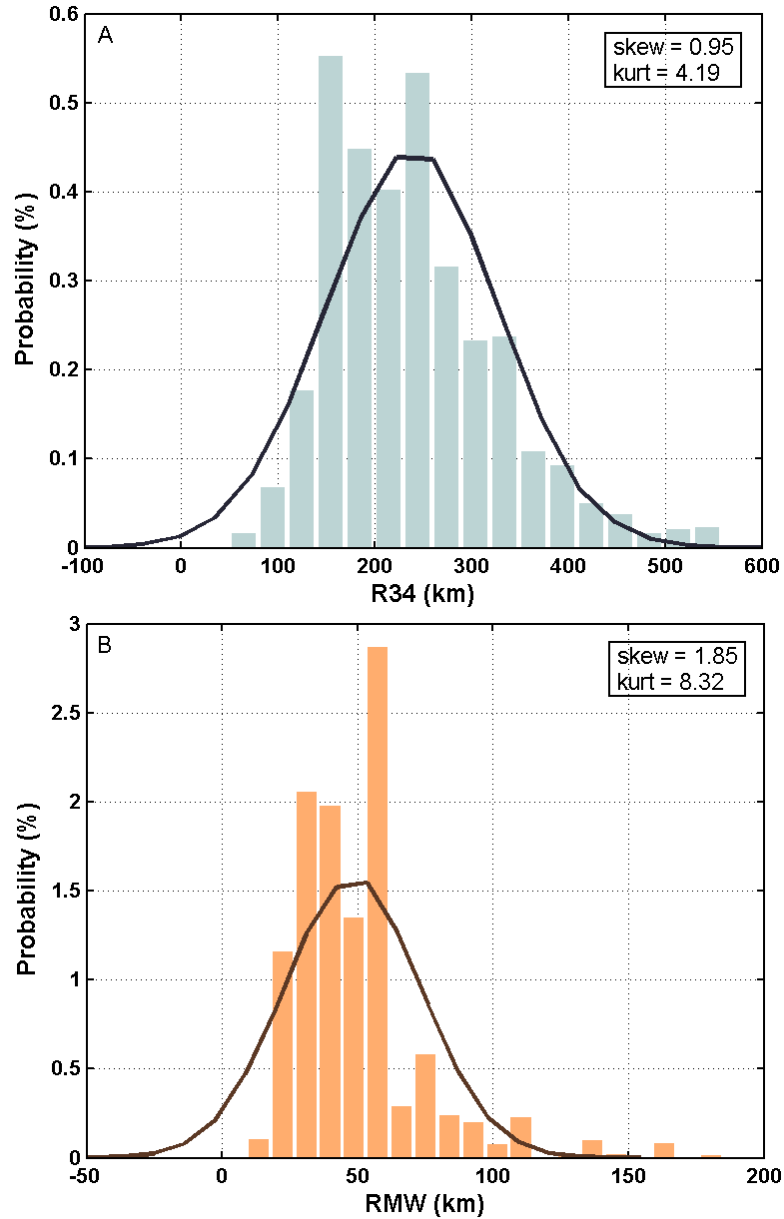


TABLE 4.5: Correlation coefficients for IKE, ACE, PD, and PDI on the seasonal and storm scale. Coefficients are calculated while controlling for duration.

	Season	Storm
IKE, ACE	0.02	0.30
PD, PDI	0.20	0.48**

FIGURE 4.4: PDF of R34 (A, blue) and RMW (B, orange) in kilometers (bars) compared to theoretical normal distributions (line) with the same mean and standard deviation. Skewness and kurtosis of the data distributions are labeled in the upper right hand corner.



seasonal climatology studies, the inclusion of size is important and necessary to fully understand the variability of tropical cyclone energetics.

In deriving PDI, Emanuel (2005) makes the assumption that “variations in storm size would appear to introduce random errors in an evaluation of equation (4) that assumes fixed storm dimensions” (i.e. storm structure is normally distributed over a large number of observations). To test this hypothesis, the distributions of R34 and RMW, which are variables of storm structure, are compared to theoretical Gaussian distributions using the probability density function (PDF)

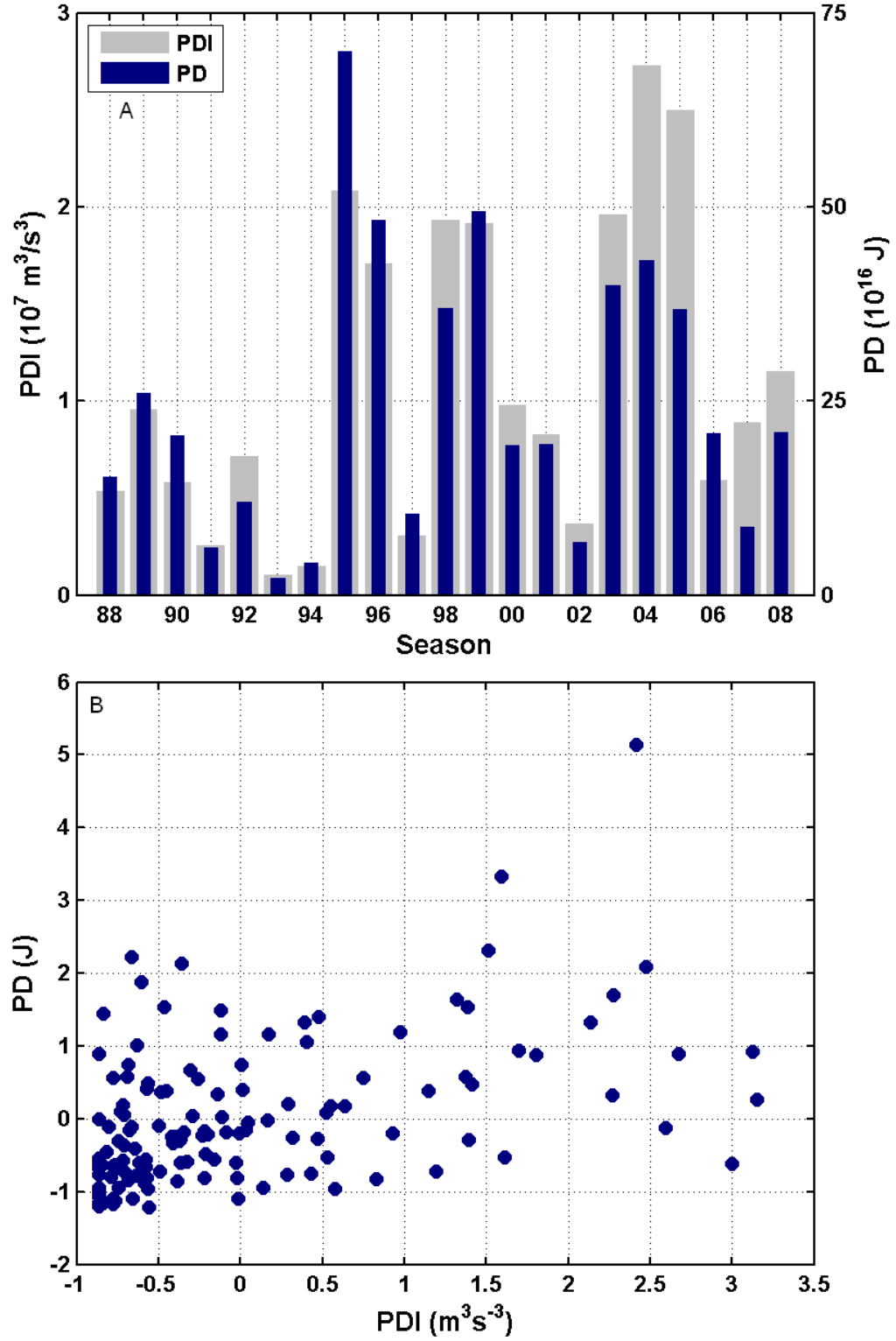
$$p(x) = \frac{1}{\sigma\sqrt{2\pi}} \exp\left(-\frac{(x-\mu)^2}{2\sigma^2}\right) \quad (17)$$

where p is the probability, μ is the mean, σ is the standard deviation, and \exp is the exponential function.

Figure 4.4 depicts the comparison between the theoretical normal distribution and the distribution of both R34 (A) and RMW (B). The distributions are not normal by a visual comparison, nor by a chi-squared test of normality. This result is strengthened when comparing the skewness and kurtosis of these distributions to normal values of 1 and 3. These moment values are indicative of a variable storm structure that is missed when a constant storm size is used in the calculation of PDI. The errors introduced in the PDI calculation due to variability in storm size are not random, and so it is suggested that PDI is not a good indicator of PD.

Figure 4.5A is the time series of PD versus PDI. Note again that the y-axes are specific to the variable, and the PDI in these figures are calculated only when storms are hurricane strength in order to be comparable to the PD calculation, analogous to the comparison between ACE and IKE (Figure 4.3). Seasons in which PDI increases and PD

FIGURE 4.5: (A) Time series of PDI (grey) and PD (blue). Y-axes are specific to the variable. (B) Comparison of storm scale PDI and PD. Values in B have been normalized and controlled for duration.



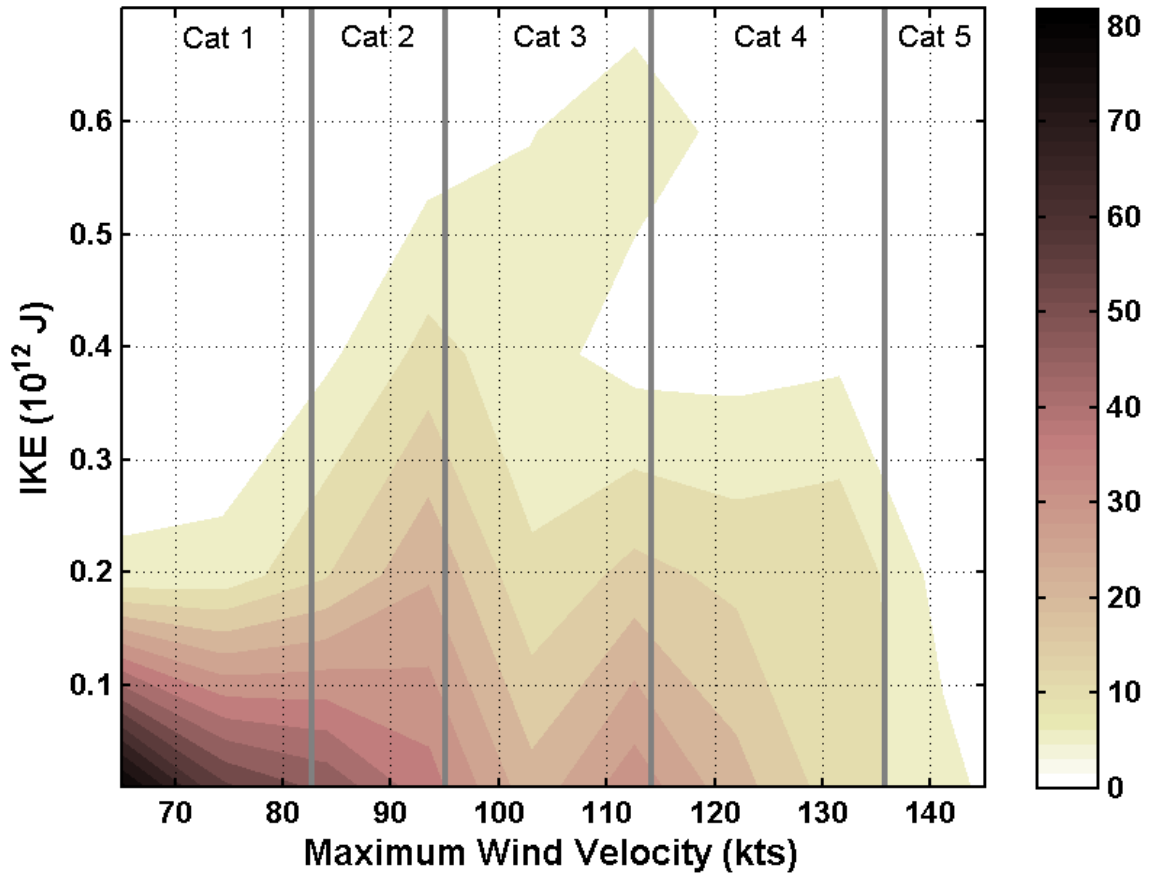
decreases, or *vice versa* are of particular interest, and exemplify the influence of radius on the seasonal scale. After standardization, the trend in PDI is 0.06, whereas the trend in PD is 0.02 (these results are true for ACE and IKE, as well). A Monte-Carlo analysis was used to test whether these trends are significantly different, and they are not. However, this is most likely due to the small number of seasons in the study (21). PDI and PD are statistically different on the seasonal time scale, with a correlation of 0.20. On the storm scale (Figure 4.5b), it is notable that the correlation between PD and PDI is larger than the correlation between ACE and IKE (Table 4.4, $R = 0.48$; significant to 99%), which is likely due to the cubed velocity term in both the PD and the PDI calculations.

Destructive Potential

The destructive potential of a storm has been difficult to predict, with category 2 and 3 storms such as Katrina (2005) and Ike (2008) doing as much, if not more, damage than Category 5 hurricanes (e.g. Camille (1969) and Andrew (1992)). The variable that has been neglected in projecting storm damage has been size.

Figure 4.6 is a joint probability density function (JPDF) between IKE and wind speed for U.S. landfalling storms from 1988 to 2008. It can be seen that category 3 hurricanes have the highest values of IKE. It is suggested that the Gulf of Mexico coastline is particularly susceptible to these occurrences for two reasons. First, the location of the Caribbean Islands and Florida play a role in the size of storms as they track from the main development region into the Gulf of Mexico. Interaction with land, although acting to decrease the intensity of the storm, also acts to extend the wind field. McWilliams (1984) studies the evolution of two-dimensional geostrophic turbulent flows

FIGURE 4.6 JPDF for U.S. landfalling storms. Shading represents the number of occurrences, and SSHS categories are labeled and partitioned over the plot in thick grey lines.



and the reaction to frictional strain. It was found that as a vortex undergoes a strain (such as a tropical cyclone undergoes when passing over a large body of land), enstrophy is transferred to larger scales. This leads the vortex to decrease in intensity while increasing the energy field. Examples of this phenomenon are Katrina (2005), Gustav (2008), and Ike (2008), where interaction with land, while weakening the cyclone intensity overall, extended the wind field and thereby the energy of the cyclone.

Second, the bathymetry in the Gulf is such that storm surge seems to play a larger role in tropical cyclone damage than wind or rain rate. Studies that attempt to model storm surges from landfalling tropical cyclones include the structure of the continental

shelf, as well as coastal geography such as bays, deltas, and barrier islands (e.g. Resio and Westerink, 2008; Jain et al. 2006). Because of its bathymetry and generally low-lying coast, the Gulf of Mexico is particularly susceptible to storm surge, which has been apparent in recent Gulf landfall events.

FIGURE 4.7: Comparison of maximum recorded surge heights to IKE (A) and maximum wind speed (B) for storms making landfall in the West Gulf region (defined in text, illustrated in Figure 4.8). Surge is in feet and maximum wind speed is in knots. Correlation in A is $R = 0.73$ ($p = 0.007$) and $R = 0.44$ ($p = 0.15$) in B.

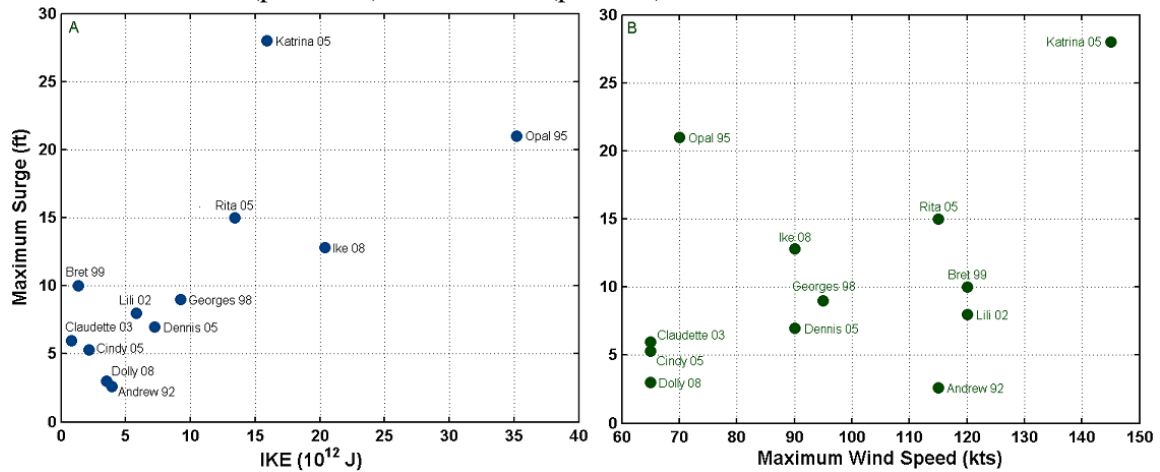
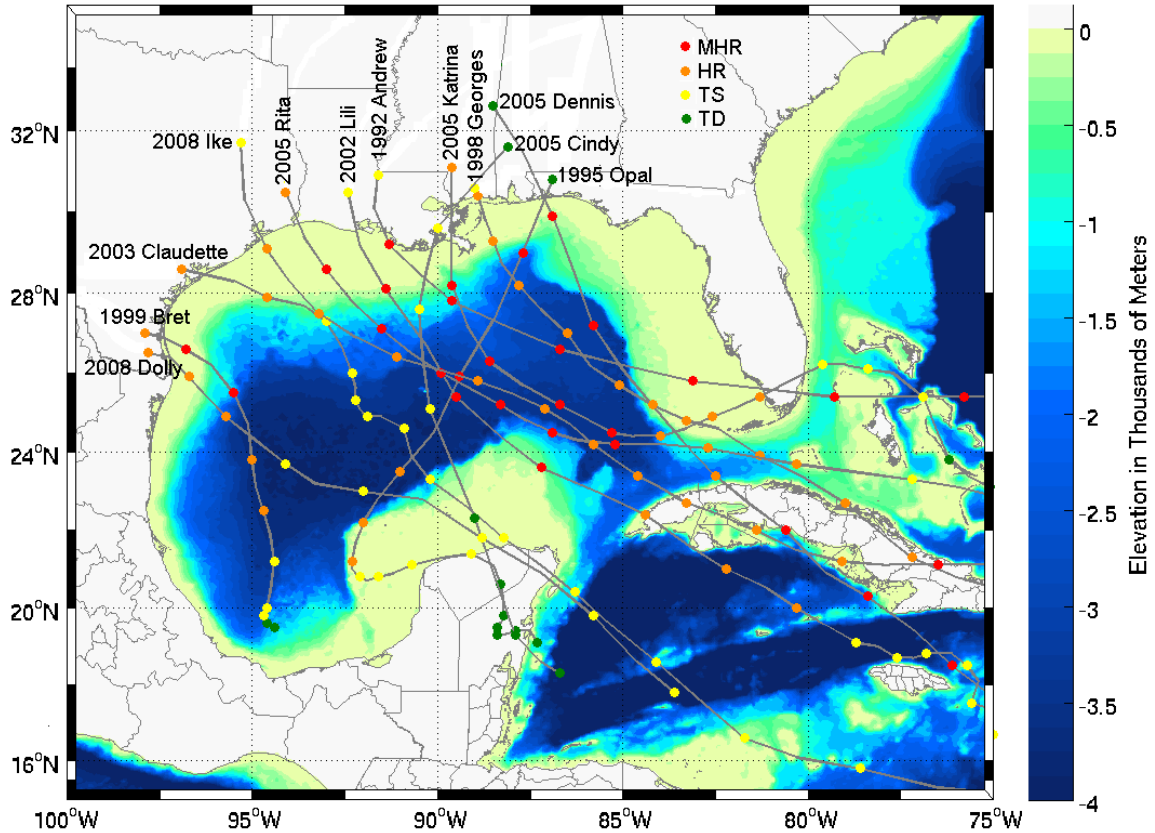


Figure 4.7A shows the relationship between mean storm IKE with the associated maximum recorded surge height for hurricanes that made landfall in the Western Gulf region, which is defined approximately from Brownsville, TX to Pensacola, FL. Storms that had surge records available in NHC storm reports were used in this analysis, and associated tracks are illustrated in Figure 4.8. The correlation between surge and IKE is $R = 0.73$, which is statistically significant with a p-value of 0.007. Given the inconsistency and general lack of storm surge reports, it is hard to draw a confident conclusion from this analysis. However, it is suggested that for storms making landfall in this region, IKE, and more generally, storm size, could be good indicators of storm surge and potential destruction more so than intensity or SSHS as shown in Figure 4.7B. The

combination of location, average storm track into the region, and bathymetry could cause this region to be particularly susceptible to large storms with high values of IKE.

FIGURE 4.8 Tracks of storms making landfall in the “West Gulf” region from 1988 to 2008. Only storms which were hurricane status upon landfall and which had recorded surge values were used. Color points represent Best Track times when the cyclone was a tropical depression (TD, green), tropical storm (TS, yellow), hurricane (HR, orange), and major hurricane (MHR, red). The grey lines are the tracks interpolated between the Best Track locations.



CHAPTER 5

CONCLUSION

This analysis has presented a method for hurricane integrated kinetic energy (IKE) that utilizes a simple, verifiable wind speed model. The model is capable of analyzing storms with minimal information (and does not require detailed wind measurements from aircraft reconnaissance) that includes only location, central pressure, maximum wind speed, and two critical radii.

The method presented in this research has been validated against AR flight-level wind speed profiles as well as the HRD kinetic energy method (Powell 2008). When compared to flight-level winds, the radial wind speed model was shown to perform well out to 75 kilometers. Furthermore, a comparison between this IKE method and times when the HRD IKE method is available shows that this model performs well, even with a lack of high-resolution wind field information.

While ACE and PDI have been the indices of choice in seasonal energy studies, it is suggested that these traditional indices be replaced with a method that accounts for the size of tropical cyclones. When compared to IKE on both the seasonal and storm scales, it has been shown that ACE and PDI are inaccurate measurements of hurricane energetics, and the assumptions that they are based on are not valid.

Furthermore, it has been shown that the storms with the largest values of IKE are only moderately strong on the SSHS and have the potential to do the most damage, as in the case of Hurricane Ike of 2008. While wind speed should be taken into account when preparing for hurricane landfall, it is important to relay the size information as well, as

this not only influences the scope of damage, but also could play a significant role in storm surge.

Improvement on the current model could be made in the following ways. First, a consistent, global, infrared-based size dataset is necessary in order to use this model for climatology studies. While the EBT data set and HURDAT are useful in the Atlantic and East Pacific regions, AR is not used in the Northern Indian Ocean, for example. Hence, it is necessary to create a tropical storm size model that uses infrared satellite information, which can then be trained and validated against AR from regions where it is available. Consistency would be of the ultimate importance in this dataset; only information that is common among all basins should be used in order to assure continuity among all years and all regions.

Lastly, given the potential of IKE as a predictor of destruction, efforts should be made to transform this method into an operational IKE forecast model. In order to do this, we must understand what controls the size of a tropical cyclone. A statistical and potentially dynamical size model can be created to essentially feed size information to the IKE method, after which IKE forecasts could be issued. These tasks are the goals of future work.

REFERENCES

- Atkinson, G. D., and C. R. Holliday, 1977: Tropical cyclone minimum sea level pressure-maximum sustained wind relationship for the western North Pacific. *Monthly Weather Review*, **105**, 421 – 427.
- Bankert, R. L., and P. M. Tag, 2002: An automated method to estimate tropical cyclone intensity using SSM/I imagery. *Journal of Applied Meteorology*, **41**, 461-472.
- Bell, G. D., and Coauthors, 2000: Climate assessment for 1999. *Bulletin of the American Meteorological Society*, **81**, S1-S50.
- Demuth, J. L., M. DeMaria, and J. A. Knaff, 2006: Improvement of advanced microwave sounding unit tropical cyclone intensity and size estimation algorithms. *Journal of Applied Meteorology and Climatology*, **45**, 1573-1581.
- Demuth, J. L., M. DeMaria, J. A. Knaff, and T. H. Vonder Haar, 2004: Evaluation of advanced microwave sounding unit tropical-cyclone intensity and size estimation algorithms. *Journal of Applied Meteorology*, **43**, 282-296.
- Depperman, C. E., 1947: Notes on the origin and structure of Phillipine typhoons. *Bull. Amer. Meteor. Soc.*, **28**, 399 – 404.
- Dvorak, V. F., 1975: Tropical cyclone intensity analysis and forecasting from satellite imagery. *Monthly Weather Review*, **103**, 420-430.
- Emanuel, K., 2005: Increasing destructiveness of tropical cyclones over the past 30 years. *Nature*, **436**, 686-688.
- Fujita, T., 1971: Proposed characterization of tornadoes and hurricanes by area and intensity. Satellite and Mesometeorology Research Project Research Paper 91, Department of the Geophysical Sciences, University of Chicago, 41 pp.
- Harper, B. A., 2002: Tropical cyclone parameter estimation in the Australian region: Wind–pressure relationships and related issues for engineering planning and design—A discussion paper. Systems Engineering Australia Party Ltd. (SEA) for Woodside Energy Ltd., SEA Rep. J0106-PR003E, 83 pp.
- Holland, G., 2008: A revised hurricane pressure-wind model. *Monthly Weather Review*, **136**, 3432-3445.
- Holland, G. J., 1980: An analytic model of the wind and pressure profiles in hurricanes. *Monthly Weather Review*, **108**, 1212-1218.

- Jain, I., P. Chittibabu, N. Agnihotri, S. K. Dube, P. C. Sinha, and A. D. Rao, 2006: Simulation of storm surges along Myanmar coast using a location specific numerical model. *Natural Hazards*, **39**, 71-82.
- Jelesnianski, C. P., J. Chen, and W. A. Shaffer, 1992: SLOSH: Sea, lake, and overland surges from hurricanes. NOAA Tech. Report NWS 48, 71 pp. [Available from NOAA/AOML Library, 4301 Rickenbacker Cswy., Miami, FL 33149.]
- Kalnay, E., and Coauthors, 1996: The NCEP/NCAR 40-year reanalysis project. *Bulletin of the American Meteorological Society*, **77**, 437-471.
- Kantha, L., 2006: Time to replace the Saffir-Simpson Hurricane Scale? *Eos, Transactions, American Geophysical Union*, **87**, 3, 6.
- Kidder, S. Q., W. M. Gray, and T. H. Vonderhaar, 1980: Tropical cyclone outer surface winds derived from satellite microwave sounder data. *Monthly Weather Review*, **108**, 144-152.
- Maclay, K. S., and M. DeMaria, 2008: Tropical Cyclone Inner-Core Kinetic Energy Evolution. *Monthly Weather Review*, **136**, 4882-4898.
- Maue, R. N., 2009: Northern Hemisphere tropical cyclone activity. *Geophysical Research Letters*, **36**.
- McWilliams, J. C., 1984: The emergence of isolated coherent vortices in turbulent flow. *Journal of Fluid Mechanics*, **146**, 21-43.
- Merrill, R. T., 1984: A comparison of large and small tropical cyclones. *Monthly Weather Review*, **112**, 1408-1418.
- Neumann, C. J., B. R. Jarvinen, C. J. McAdie, and G. R. Hammer (1999), Tropical Cyclones of the North Atlantic Ocean, 1871–1998, 206 pp., NOAA, Silver Spring, MD.
- Powell, M. D., and P. G. Black, 1990: The relationship of hurricane reconnaissance flight level wind measurements to winds measured by NOAA oceanic platforms. *Journal of Wind Engineering and Industrial Aerodynamics*, **36**, 381-392.
- Powell, M. D., and T. A. Reinhold, 2007: Tropical cyclone destructive potential by integrated kinetic energy. *Bulletin of the American Meteorological Society*, **88**, 513-+.
- Powell, M. D., S. H. Houston, L. R. Amat, and N. Morisseau-Leroy, 1998: The HRD real-time hurricane wind analysis system. 53-64.
- Resio, D. T., and J. J. Westerink, 2008: Modeling the physics of storm surges. *Physics Today*, **61**, 33-38.

Schloemer, R. W., 1954: Analysis and synthesis of hurricane wind patterns over Lake Okechobee, FL. Hydromet Rep. 31, 49 pp. [Govt. Printing Office, No. C30.70:31].

Weatherford, C. L., and W. M. Gray, 1988a: TYPHOON STRUCTURE AS REVEALED BY AIRCRAFT RECONNAISSANCE .1. DATA-ANALYSIS AND CLIMATOLOGY. *Monthly Weather Review*, **116**, 1032-1043.

U.S. Department of Commerce, 2009: National Hurricane Operations Plan. FCM-PI2-1995. Office of the Federal Coordinator for Meteorological Services and Supporting Research, NOAA. 160 pp.